Environmental Science & Technology

Article

pubs.acs.org/est

Temporal Characteristics of Brown Carbon over the Central Indo-Gangetic Plain

Rangu Satish,[†] Puthukkadan Shamjad,[‡] Navaneeth Thamban,[‡] Sachchida Tripathi,[‡] and Neeraj Rastogi*,[†]

[†]Geosciences Division, Physical Research Laboratory, Ahmedabad 380009, India

[‡]Department of Civil Engineering and Centre for Environmental Science and Engineering, Indian Institute of Technology-Kanpur, Kanpur 208016, India

Supporting Information

ABSTRACT: Recent global models estimate that light absorption by brown carbon (BrC) in several regions of the world is ~30−70% of that due to black carbon (BC). It is, therefore, important to understand its sources and characteristics on temporal and spatial scales. In this study, we conducted semicontinuous measurements of water-soluble organic carbon (WSOC) and BrC using particle-into-liquid sampler coupled with a liquid waveguide capillary cell and total organic carbon analyzer (PILS-LWCC-TOC) over Kanpur (26.5°N, 80.3°E, 142 m amsl) during a winter season (December 2015 to February 2016). In addition, mass concentrations of organic and inorganic aerosol and BC were also measured. Diurnal variability in the absorption coefficient of BrC at 365 nm (b_{abs_365}) showed higher values (35 ± 21 Mm^{-1}) during late evening to early morning hours and was attributed to primary emissions from biomass burning (BB) and fossil fuel burning (FFB). The b_{abs_365} reduced by more than 80% as the day progressed, which was ascribed to photo bleaching/volatilization of BrC and/or due to rising boundary layer height. Further, diurnal variability in the ratios of b_{abs_405}/b_{abs_365} and b_{abs_420}/b_{abs_365} suggests that the BrC composition was not uniform throughout a day. WSOC exhibited a strong correlation with b_{abs_365} (slope = 1.22 ± 0.007, r^2 = 0.70, n = 13 265, intercept = −0.69 ± 0.17), suggesting the presence of a significant but variable fraction of chromophores. Mass absorption efficiency (MAE) values of WSOC ranged from 0.003 to 5.26 $m^2\ g^{-1}$ (1.16 ± 0.60) during the study period. Moderate correlation (r^2 = 0.50, slope = 1.58 ± 0.019, n = 6471) of b_{abs_365} was observed with the semivolatile oxygenated organic aerosols (SV-OOA) fraction of BB resolved from positive matrix factorization (PMF) analysis of organic mass spectral data obtained from a high-resolution time-of-flight aerosol mass spectrometer (HR-ToF-AMS). The low-volatility OOA (LV-OOA) fraction of BB had a similar correlation to b_{abs_365} (r^2 = 0.54, slope = 0.38 ± 0.004, n = 6471) but appears to have a smaller contribution to the absorption.

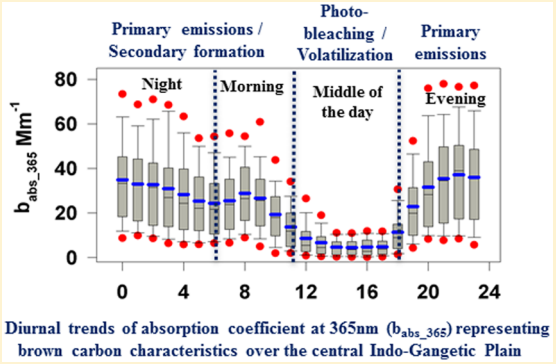

Diurnal trends of absorption coefficient at 365nm (b_{abs_365}) representing brown carbon characteristics over the central Indo-Gangetic Plain

1. INTRODUCTION

Carbonaceous aerosols, composed of organic carbon (OC) and black carbon (BC), are ubiquitous in the atmosphere.[1] A significant fraction (20−80%) of organic aerosol (OA) is reported to be water-soluble, which can promote cloud formation and thus affects climate cooling and the hydrological cycle.[2] On the contrary, BC has been shown to exhibit a positive effect on radiative forcing due to its light-absorbing property. Until recent years, BC was the only known light absorbing carbonaceous component in atmospheric aerosol and the organic portion was considered to be only a scattering component. Recently, many field observations and chamber studies have shown that a certain fraction of OC can also absorb solar radiation, especially in the near UV and visible regions.[3−6] This fraction of OA that absorbs light at near UV to visible regions is termed as brown carbon (BrC).[7] Climatic significance of BrC through direct radiative forcing (DRF) is an important issue. Further, there is a semidirect effect causing significant warming/heating of cloud droplets due to the presence of both BC and BrC, which could lead to cloud dissipation/evaporation.[7]

Global simulations suggest that a strongly absorbing BrC contributes up to +0.25 W m^{-2} (or 19%) of the absorption by absorbing anthropogenic aerosols.[8] Regional effects of DRF of BrC over major areas of biomass burning (BB) and biofuel combustion, such as South and East Asia, South America, and subtropical Africa, may be substantially higher than 0.25 W m^{-2}, suggesting BrC may be a significant atmospheric light absorbing species in these regions.[8] Over the Indo-Gangetic Plain (IGP), DRF of BrC showed the monthly warming effect up to 0.5 W m^{-2} during the spring season.[9] A recent global

Received: February 23, 2017
Revised: May 17, 2017
Accepted: May 18, 2017
Published: May 18, 2017

DOI: 10.1021/acs.est.7b00734
Environ. Sci. Technol. 2017, 51, 6765−6772

model estimates that atmospheric absorption by BrC ranges from +0.22 to +0.57 W m^{-2}, which corresponds to 27− 70% of that predicted due to BC.[10]

OC is composed of a wide variety of organic species including primary oxygenated organics such as humic like substances (HULIS), which are similar to terrestrial and aquatic humic and fulvic acids.[11] Further, water-soluble organic carbon (WSOC) predominantly consists of a secondarily formed oxygenated organic aerosol.[12] Laboratory studies have demonstrated that secondary BrC can be produced from a variety of atmospheric aging processes that often involve nitrogenous compounds.[13−15] All or a fraction of WSOC can be light absorbing depending upon its composition. Further, both fossil fuel burning (FFB) and BB emissions could be significant sources of BrC (or its precursors) in the atmosphere.[7] However, knowledge of the major sources and characteristics of BrC vary on temporal and spatial scale is sparse in the literature, which is important in assessing BrC effects on climate.

The IGP is home to about 1 billion inhabitants and spread over 700 000 km^2 of area stretching from the plains of the Indus River in Pakistan to the plains of the Ganges River in India and Bangladesh. Agriculturally the "bread basket" of South Asia, ∼120 000 km^2 of land area is used for growing rice, wheat, and major cereal crops.[16] The IGP region over northern India receives a large amount of primary particles and precursors of secondary particles from vehicles, industries, large-scale postharvest BB, and biofuel burning during winter.[17−19] Carbonaceous aerosols from anthropogenic sources are of considerable significance in the regional atmospheric chemistry and climate change scenario over the Indian subcontinent.[20]

This paper mainly focuses on the temporal characteristics of BrC (defined in section 2) over the IGP under the influence of different sources (BB, FFB, and long-range transport) and meteorological conditions using first-ever semicontinuous measurements of BrC in India. Further, positive matrix factorization (PMF) analysis was conducted on the organic mass spectral data obtained from the HR-ToF-AMS. The factors resolved from this analysis were then compared with the light-absorbing properties of the aerosol (mostly b_{abs_365}) measured by the PILS-LWCC-TOC in order to see which factor (or type of OA) may explain the BrC features measured over the study region.

2. EXPERIMENTAL SECTION

2.1. Site Description. Semicontinuous measurements of water-soluble BrC (hereafter termed as BrC, defined in section 2.2.1) were carried out at a site located on the campus of Indian Institute of Technology, Kanpur (26.5°N, 80.3°E, 142 m above mean sea level) during the 20th of December, 2015 to the 6th of February, 2016. Being located in the middle of the IGP, Kanpur is a big urban city with a population of ∼4.5 million and reported to be among cities with the worst air quality in India.[21,22] The sampling site receives emissions from several sources in and around the city and from the north and northwestern IGP through long-range transport. During winter, regional BB is among the major contributors to aerosol loadings at this location.[23] Other sources of pollution in the Kanpur city are emissions from vehicles, biofuel, wood and coal burning, industrial activities, brick kilns, and thermal power plant plumes.[24] Further, meteorological conditions in winter (low wind speeds and shallow boundary layer heights) favor the accumulation of pollutants over the region. The study period was characterized by high RH (up to 100%) and low temperature conditions (lowest temperature: approximately 4 °C).

2.2. Sampling and Analysis. *2.2.1. Semicontinuous Measurements of BrC and WSOC.* For the measurements of BrC present in WSOC, many studies have used traditional UV−vis spectrometric techniques.[25−27] Some studies have used UV−vis and fluorescence spectroscopy to characterize the brownness of organic compounds.[28] In this study, we used a spectrometric technique adopted from Hecobian et al.[4] BrC absorption spectra (300−800 nm) and WSOC mass concentration in ambient $PM_{2.5}$ have been measured semicontinuously using an assembled system (PILS-LWCC-TOC) consisting of a particle-into-liquid sampler (PILS, Model ADI 2081, Applicon Analytical) coupled to a liquid waveguide capillary cell (LWCC, World Precision Instrument, Sarasota, FL, 2m path length) and total organic carbon (TOC, Sievers 900 Portable with Turbo, GE Analytical Instruments) analyzer. The ambient air was drawn through a cyclone inlet ($PM_{2.5}$ URG, model no. URG-2000-30EH) coupled to a PILS-LWCC-TOC system at 16.7 lpm airflow rate. Aerosol water-extract from the sample line coming out of PILS was passed through a disposable syringe filter (with GHP Membrane, 0.45 μm porosity, 25 mm diameter, Acrodisc) to remove all of the insoluble particles (including BC) prior to injecting it in LWCC and TOC analyzers. The BrC absorption spectra (300−800 nm) were measured using a portable UV−vis spectrophotometer (model USB-4000) and deuterium and tungsten halogen lamps (DT-Mini-2, Ocean Optics) and saved every 2 min, whereas WSOC concentrations were measured with 4 min integration time. The PILS-LWCC-TOC system setup was similar to that reported by Hecobian et al.[4] Background measurements were performed everyday by putting a high-efficiency particulate air (HEPA) filter to the cyclone inlet for about 1 h, and reported concentrations are corrected for blanks.

Details of the semicontinuous measurement of WSOC have been described by Rastogi et al.[29] In the present study, the light absorption coefficient at a given wavelength (b_{abs_λ}) was calculated as follows (as described in Hecobian et al.[4])

$$b_{abs\_\lambda} = (A_\lambda - A_{700})\left(\frac{V_l}{V_a l}\right)\ln 10 \quad (1)$$

where A_λ is the absorbance at a given wavelength, A_{700} is the absorbance at 700 nm to account for any baseline drift, V_l is the PILS liquid sample flow rate (0.7 mL min^{-1}), and V_a is the air sampling flow rate (16.7 L min^{-1}). The absorbing path length "l" is 2 m. Using b_{abs_365} (Mm^{-1}) and WSOC ($\mu g\ m^{-3}$), the mass absorption efficiency (MAE, $m^2\ g^{-1}$) was calculated as follows:

$$\mathrm{MAE} = \frac{b_{abs\_365nm}}{\mathrm{WSOC}} \quad (2)$$

MAE is a key parameter that describes the total light absorbing ability of all of the chromophores present in aerosol water extract. In this study, absorption coefficient at 365 nm (b_{abs_365}) was used as a general measure of the absorption by BrC. This wavelength was chosen because it is far enough from the UV region to avoid interferences from nonorganic compounds (e.g., nitrate); HUMIC like substances (HULIS) absorb at this wavelength, and it is similar to that used in other studies.[4,30] It is important to note that all WSOC may or may not be BrC, as

DOI: 10.1021/acs.est.7b00734
Environ. Sci. Technol. 2017, 51, 6765−6772

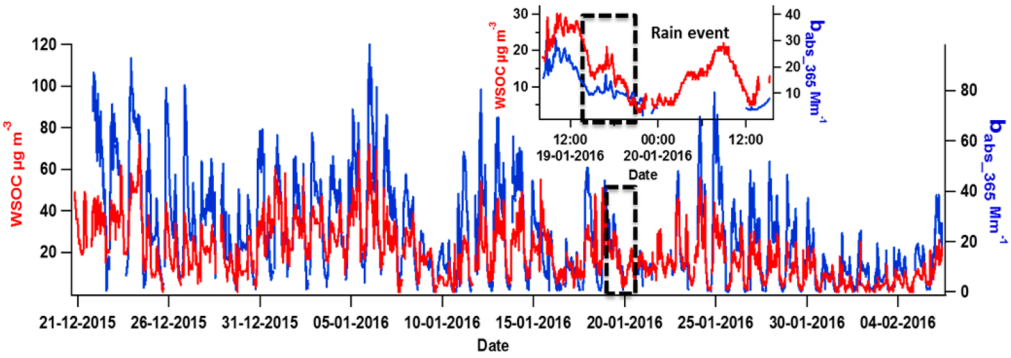

Figure 1. Temporal variability in WSOC (μg m^{-3}) concentration and BrC absorption coefficient (b_{abs_365}, Mm^{-1}) during the study period. The inset figure shows the temporal variability of these species before, during, and after a rain event occurred on January 19th.

BrC is a fraction of WSOC that can be anywhere between zero to one. Therefore, the reported MAE of WSOC shall be considered as the lower limit of water-soluble BrC.

2.2.2. Semicontinuous Measurements of Chemical Species. Chemical composition of atmospheric submicron aerosol was also characterized semicontinuously with a high-resolution time of flight aerosol mass spectrometer (HR-ToF-AMS, Aerodyne Research Inc., USA) during the 27th of December, 2015 to the 7th of February, 2016, with 2 min of integration time. The HR-ToF-AMS measures sulfate, nitrate, ammonium, chloride, and total organic aerosol (OA) in nonrefractory PM_1 ($NR\text{-}PM_1$). HR-ToF-AMS is also capable of separating the signals from various ions at each minimal m/z which are further classified into various fragment families based on atoms contained in each ion.[31] Cx and CH are less oxidized CxHy (hydrocarbon) family, while CHO and CHOgt1 (CHO > 1) are the oxygenated families of organic fragments containing one and more than one oxygen, respectively.[32,33] CHOgt1N (CHO > 1N) are more oxygenated nitrogen containing organic fragments of general formulas $C_XH_YO_ZN_W$ where $x \geq 1$, $y \geq 0$, $z \geq 1$, $w \geq 1$. An aethalometer (AE 42, Magee Scientific) was used to measure the BC concentrations at seven different wavelengths with 5 min integration time. Carbon monoxide (CO) and oxides of nitrogen (NO_X, i.e., NO + NO_2) were measured using gas analyzers (Serinus, Ecotech) with 2 min integration time.

3. RESULTS AND DISCUSSION

3.1. Temporal Variability of WSOC and BrC. Figure 1 depicts a large diurnal and day-to-day variability in WSOC concentration and b_{abs_365} values. The WSOC varied from 1.0 to 72 μg m^{-3} (avg ± sd: 20 ± 13, 1σ) and b_{abs_365} ranged from 0.02 to 98 Mm^{-1} (24 ± 19) during the study period. This variability is attributable to various factors such as dominance of specific sources (BB, FFB), atmospheric processes such as long-range transport, transformation, secondary organic aerosol (SOA) formation, and meteorological conditions over the central IGP. The possible role of these factors is discussed in subsequent text. Concentrations of gaseous species (CO, NO_X), inorganic ions (NH_4^+, NO_3^-, SO_4^{2-}, and Cl^-), and AMS mass fragments of organic components (CH, CHO, CHO > 1, CHO > 1N, CHON) also exhibited large variability during the study period (Figure S1), which was broadly similar to that of WSOC and b_{abs_365}. Further, concentrations of all of the measured species were relatively high with considerable fluctuations during December and January and subsequently subsided in February. Here, December and January months are characterized by the lowest temperature, and subsequently, the temperature starts rising in February which changes the boundary layer height. Winds also become stronger during February which enhances species removal from the study site.[34] Further, there was relatively high aerosol loading during the nighttime, which is attributable to the shallower boundary layer height (Figure S2c). The lowest concentrations of all of the species including WSOC and b_{abs_365} were observed during a rain event that occurred on January 19th (Figure 1), which had cleaned the atmosphere. However, the atmosphere was loaded again quickly with significant concentrations of various chemical species within a few hours after the rain event, suggesting local sources were very active.

WSOC exhibited a strong correlation with b_{abs_365} (slope = 1.22 ± 0.007, r^2 = 0.70, n = 13 265, intercept = −0.69 ± 0.17, Figure 2a), suggesting that a significant fraction of WSOC is BrC chromophores, which are absorbing at 365 nm. Here (and everywhere in the text), the slope is given with standard error. Further, MAE (as defined in eq 2) ranged from 0.003 to 5.26 m^2 g^{-1} (1.16 ± 0.60) during the study period. The average MAE value (1.16) is higher in comparison to those documented in the literature such as 0.60 over South Deklab, U.S.A.,[4] 0.73 over Pasadena, U.S.A.,[35] and 0.75 (daytime) and 1.13 (nighttime) over Patiala, India,[36] and lower in comparison to values reported over Delhi (1.6)[37] and Beijing (1.8).[38] These observations suggest that the study region (including Patiala and Delhi) has higher abundances and/or higher absorbing capacity of BrC chromophores in comparison to those reported over different sites in the U.S.A., whereas lower than that documented over Beijing, China.

Large variability in MAE (0.003 to 5.26 m^2 g^{-1}) could be due to various reasons such as different types of BrC species have different absorption properties, and their abundances are changing with time under different meteorological conditions. These chromophores could be primary and/or secondary BrC species from BB and/or FFB emissions with different absorption properties. Certain meteorological conditions may also reduce/enhance the absorption properties of BrC chromophores. To investigate and understand this variability, the data have been investigated in different ways.

Hours of the day are shown in the colored scale in Figure 2a. To understand the diurnal variability in the characteristics of BrC (Figure 2b), the data have been spilt into three time periods, A: 18:00−06:00 h (evening + night), B: 06:00−11:00 h (morning), and C: 11:00−18:00 h (middle of the day), respectively, as the b_{abs_365} data points corresponding to these time periods appear to follow similar characteristics (Figures

DOI: 10.1021/acs.est.7b00734
Environ. Sci. Technol. 2017, 51, 6765−6772

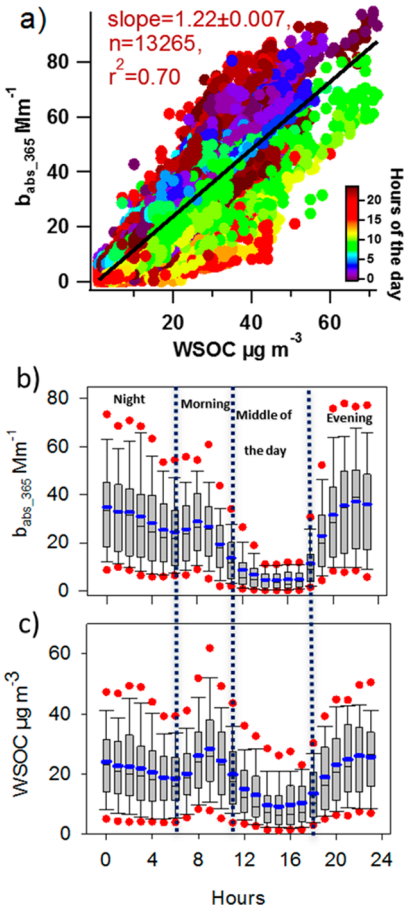

Figure 2. (a) Scatter plot between WSOC (μg m^{-3}) and b_{abs_365} (Mm^{-1}), (b) box-whisker plot showing diurnal trends of b_{abs_365}, and (c) box-whisker plot showing diurnal trends of WSOC. The boundary of the box closest to zero indicates the 25th percentile, black and blue lines within the box represent median and mean, respectively, and the boundary of the box farthest from zero indicates the 75th percentile. Error bars above and below the box indicate the 90th and 10th percentiles. Red circles are indicative of outliers.

2a,b). A noticeable difference was observed in the MAE of WSOC for the periods A (slope = 1.34 ± 0.01, r^2 = 0.76, n = 7181), B (slope = 0.95 ± 0.01, r^2 = 0.72, n = 3223), and C (slope = 0.58 ± 0.01, r^2 = 0.62, n = 2975) (Figure S3), reflecting the change in absorbing properties of BrC at different times of the day. Here, the slopes are given with standard errors. The highest slope (representing MAE of WSOC) was observed for the data points corresponding to period A and attributed to active primary sources, as corresponding H:C ratios (from HR-ToF-AMS) were relatively high during these hours (discussed later). To understand the role of primary emissions on BrC characteristics, CO is also used as tracer of emissions from primary sources.[4] A reasonably good correlation (r^2 = 0.48, n = 12272) between b_{abs_365} and CO was observed (Figure S4), suggesting primary emissions are a significant source of BrC (or its precursors) over the study region. The second highest MAE of WSOC was observed for the period B, possibly due to the influence of active primary sources and secondary formation of BrC. A substantial increase in WSOC/CO ratio was observed during period B, which is suggestive of SOA formation.[4,25] Both WSOC and b_{abs_365} increased rapidly during sunrise, which contrasts with that observed by Hecobian et al.[4] When both WSOC and b_{abs_365} were high along with CO, the WSOC/CO and b_{abs_365}/CO ratios are expected to be low; however, if these ratios were high then it would indicate that there are multiple sources of these species (other than primary emissions) with different source strengths. The WSOC/CO and b_{abs_365} /CO ratios were low when local burning sources were present. Lowest MAE of WSOC was observed during period C (slope = 0.58 ± 0.01, r^2 = 0.62, n = 2975), when BrC continued to decrease with increasing sunlight exposure. Middle of the day b_{abs_365} values (6 ± 5) were ∼80−90% lower than those during nighttime (35 ± 21, Figure 2b). This observation suggests that either daytime secondarily formed BrC is less absorbing, and/or ambient BrC goes through photo bleaching during daytime, or it is volatile and evaporates with increasing temperature during daytime (Figure S2b, discussed later).[39,40,15] Expanded boundary layer height during daytime would also reduce b_{abs_365} values. However, the exact reason (s) for the decrease in b_{abs_365} values during the day remains unclear, especially since measurements for these potential degradation or dilution processes are lacking in this study.

3.2. Diurnal Variability in BrC Chromophores. BrC is characterized by an absorption spectrum that smoothly increases from the visible to UV wavelengths.[7] The BrC absorption at 365 nm has been shown to be mainly associated with HULIS compounds;[30] however, other chromophores may peak at different wavelengths.[38,41] The absorption observed at different wavelengths may or may not change uniformly throughout the day as the chromophore composition may or may not be constant all of the time. Different types of chromophores can be emitted from various sources and/or formed in the atmosphere. Budisulistiorini et al.[6] have shown that the direct burning of several types of biomass can produce primary BrC. Recent laboratory studies have found that anthropogenic VOCs (benzene, toluene, phenols, and polycyclic aromatic hydrocarbons (PAHs)) react with nitrogen oxides and produce nitro aromatics.[13,14,27] Nitrophenols and nitrocatechols have been identified as dominant light-absorbing compounds in cloudwater samples, and in $PM_{2.5}$ particles impacted by BB and FFB.[42,43]

In the present study, absorptions at 405 nm (representing 2,4-dinitrophenol) and 420 nm (representing 3-nitrophenol) were selected to compare with 365 nm (representing HULIS).[43] It is expected that spectral absorbance would be different at different times of the day if BrC composition is not uniform. Ratios of b_{abs_405}/b_{abs_365} and b_{abs_420}/b_{abs_365} were investigated to understand whether BrC composition was uniform during the study period and/or whether there was any diurnal variability in BrC composition over the study site. Absorption ratios of b_{abs_405}/b_{abs_365} and b_{abs_420}/b_{abs_365} exhibited considerable variability at different times of the day (Figure 3a,b), suggesting BrC composition was not uniform. The ratios were minimum during afternoon (14:00 to 17:00), more or less similar during evening and night hours, and exhibit a small positive hump during morning rush hours (08:00 to 10:00; Figures 3a, b). Interestingly, the diurnal trends in b_{abs_405}/b_{abs_365} and b_{abs_420}/b_{abs_365} during rush hours were similar to that exhibited by organic compounds of CHO > 1N family (Figure 3c). It implies that considerable fraction of BrC chromophores could be nitrogen-containing organic compounds over the study region and likely they are volatile and/or affected by photobleaching (as ratios were minimum during afternoon hours, Figures 3 and S2b). These observations also suggest that BrC chromophores are a variable mixture of at least HULIS and nitrogen-containing organic compounds over

DOI: 10.1021/acs.est.7b00734
Environ. Sci. Technol. 2017, 51, 6765−6772

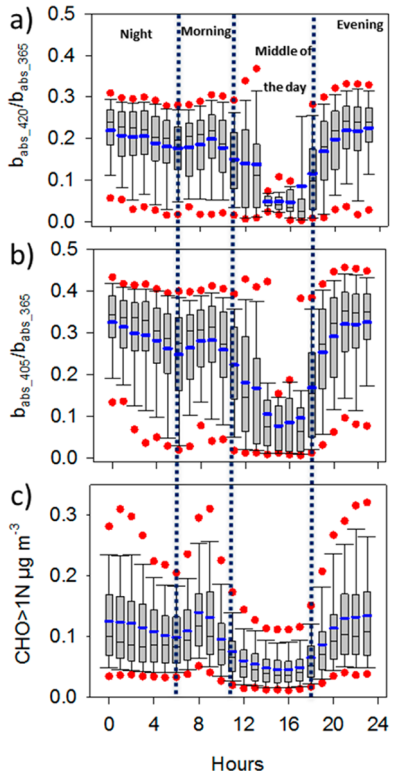

Figure 3. Box-whisker plots showing diurnal trends of (a) b_{abs_420}/b_{abs_365}, (b) b_{abs_405}/b_{abs_365}, and (c) CHO > 1N (μg m^{-3}). For the details of lines and symbols, refer to caption of Figure 2. Here, CHO > 1N are more oxygenated (more than one oxygen) nitrogen containing organic fragments of the general formula $C_xH_yO_zN_w$ where $x \geq 1$, $y \geq 0$, $z \geq 1$, and $w \geq 1$.

the study region, and BrC absorption properties at a given time depend upon the type of chromophores and meteorological parameters.

3.3. Effect of Meteorological Conditions on BrC. Atmospheric BrC species are susceptible to photochemical degradation, as their optical properties can be altered by aqueous-phase photochemical processing with both photo-enhancement and photobleaching processes.[39] In this study, the b_{abs_365} depicted photoenhancement during early hours after sunrise possibly due to aqueous-SOA formation as WSOC also increased at this time. BrC absorption diminished during the middle of the day (Figure 2b), likely due to photodissociation and/or due to the volatile nature of BrC, as the temperature went to maximum during this time (Figure S2b). The lower BrC could also be due to the fact that planetary boundary layer (PBL) heights was also highest during middle of the day (Figure S2c). Zhao et al.[15] had documented that the presence of oxidants like O_3 and OH radicals (abundant during daytime) may degrade BrC into smaller and more volatile organic compounds. Higher absorption during evening to night is attributable to primary sources as well as shallow boundary layer height (Figure S2c), and the absence of volatilization and photobleaching processes.

3.4. Characteristics of BrC from Different Sources. PMF analysis was performed on the V-mode high-resolution data of AMS organic mass spectra, where the OA was further divided into several factors based on their characteristics (details are given in the Supporting Information, Figure S5, S6, S7, S8). These factors include low-volatility oxygenated OA (LVOOA-1 and LVOOA-2), semivolatile oxygenated OA with significant contribution from biomass burning organics (SVOOA-BBOA-1 and SVOOA-BBOA-2), hydrocarbon-like OA (HOA), and biomass burning OA (BBOA). Source profiles of these factors are presented in Figure S6, and details of these factors are given in Supporting Information. To understand the relation and relative source contribution of different OA factors to BrC absorption, these factors are plotted against b_{abs_365} (Figure 4). In the same figure, the WSOC/OA ratio is also used as a colored axis to understand the effect of these factors on BrC as a function of their solubility in water. Here, WSOC data is from PILS-TOC and OA is from HR-ToF-AMS. It is noteworthy that WSOC/OA ratios are used rather than water-soluble organic matter (WSOM)/OA ratio to avoid uncertainty

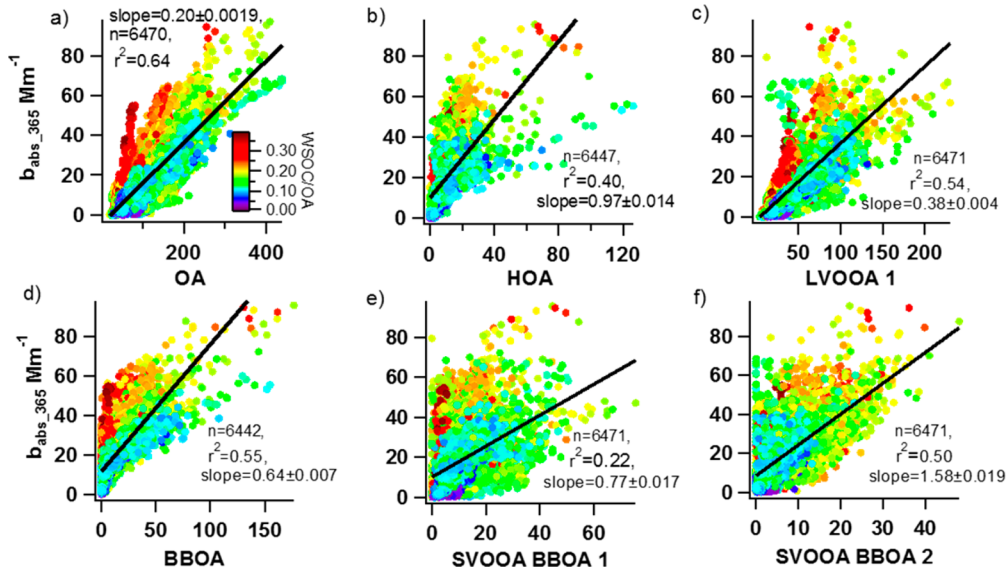

Figure 4. Linear regressions analysis of b_{abs_365} (Mm^{-1}) with PMF derived factors (μg m^{-3}) like (a) organic aerosol (OA), (b) hydrocarbon like OA (HOA), (c) low volatile oxygenated OA 1 (LVOOA1), (d) biomass burning OA (BBOA), (e) semi volatile oxygenated OA biomass burning OA 1 (SVOOA BBOA 1), and (f) semi volatile oxygenated OA biomass burning OA 2 (SVOOA BBOA 2).

DOI: 10.1021/acs.est.7b00734
Environ. Sci. Technol. 2017, 51, 6765−6772

associated with WSOM, which requires an assumed constant factor to be multiplied to WSOC. On average, the WSOC/OA ratio was 0.14 ± 0.06 during the study period.

Total OA shows a very strong correlation with WSOC (slope = 0.17 ± 0.001, r^2=0.79, n = 7380, Figure S9). Total OA also exhibits a strong linear regression with b_{abs_365} (slope = 0.20 ± 0.002, r^2=0.64, n = 6470, Figure 4a), and the slope of this regression is expected to be a weighted average of the slopes of b_{abs_365} with different PMF fractions of OA. The order of slopes was SVOOA-BBOA-2 (1.58 ± 0.019) > HOA (0.97 ± 0.014) > SVOOA-BBOA-1 (0.77 ± 0.017) > BBOA (0.64 ± 0.007) > LVOOA-1 (0.38 ± 0.004), which indicate the absorption capacity of BrC from respective source factors. One factor (LVOOA-2) had not shown a good correlation (r^2 = 0.05) with b_{abs_365}. It infers that oxidized or aged OA does not absorb considerably, as LVOOA-2 consists of highly oxidized organic species (Figure S6f). The PMF factors of OA aerosol from BB origin are BBOA, SVOOA-BBOA-1 and SVOOA-BBOA-2. Here, b_{abs_365} showed a good correlation with BBOA (slope = 0.64 ± 0.007, r^2 = 0.55, n = 6442, O/C = 0.26) and SVOOA-BBOA-2 (slope = 1.58 ± 0.019, r^2 = 0.50, n = 6471, O/C = 0.43), but not with SVOOA-BBOA-1 (slope = 0.77 ± 0.017, r^2 = 0.22, n = 6471, O/C = 0.55); it further suggests that more oxidized OA are less absorbing in nature.[45] Such an observation also suggests that primary BB emissions produce strongly absorbing BrC (as also documented by Budisulistiorini et al.[6]), which include a large contribution from semivolatile species (SVOOA-BBOA-2). Further, SVOOA-BBOA-2 also consists of highest N/C (0.07) ratio among all OA factors (Figure S6d), suggesting that nitrogenous compounds enhance the absorbing capacity of the OA. However, abundance of both b_{abs_365} and SVOOA-BBOA-2 reduces during daytime when temperature increases, suggesting photochemical oxidation and/or volatilization of SVOOA-BBOA-2 in the atmosphere reduces BrC absorbing capacity, as discussed in previous section. Further, the hydrocarbon type primary OA (or HOA) exhibited considerable linearity with BrC absorption (slope = 0.97 ± 0.014, r^2 = 0.40, n = 6447), suggesting primary sources are significant contributor to light-absorbing OA over the study region. Lowest slope was observed with LVOOA-1 (slope = 0.38 ± 0.004, r^2 = 0.54, n = 6471), further indicating that aging or oxidation of organics reduces their light absorption capability. This result has important implications in predicting the light absorbing capability of OA based on its PMF derived factors. Further, higher b_{abs_365} values for data points with higher WSOC/OA ratios suggest that water-soluble chromophores from respective sources are relatively more absorbing (Figure 4).

4. ENVIRONMENTAL IMPLICATION

BrC immersed in cloud droplets can absorb light and facilitate evaporation/dispersion of clouds.[7] It contributes ∼35% of the direct radiative forcing warming by carbonaceous aerosols.[44] However, in order to assess the effects of BrC on air quality and climate, a proper understanding of its sources and characteristics on temporal and spatial scales is very important. This study reports BrC absorption properties, their major sources, and their characteristics over the central Indo-Gangetic Plain through wide variety of semicontinuous measurements. It also indicates the possible effects of meteorological conditions on BrC characteristics. Primary emissions from biomass burning (BB) and fossil fuel burning (FFB) are the major sources of highly absorbing BrC. Secondary BrC and aged/oxygenated OA are relatively less absorbing. Further, BrC absorption decreases as the day progresses achieving a minimum during afternoon hours. It is also shown that BrC composition is not uniform throughout the day. Our observations suggest that BrC chromophores are a variable mixture of at least HULIS and nitrogen containing organic compounds over the study region. These results have implications in regional radiation budget. They may also be useful in understanding wintertime fog formation and dissipation processes over the central IGP. This study qualitatively depicts the possible role of meteorological parameters on the abundances of BrC, which may be useful in assessing meteorological effects on similar atmospheric species.

■ ASSOCIATED CONTENT

Supporting Information

The Supporting Information is available free of charge on the ACS Publications website at DOI: 10.1021/acs.est.7b00734.

Figures S1−S9 and detailed description of positive matrix factorization (PMF) analysis (PDF)

■ AUTHOR INFORMATION

Corresponding Author

*E-mail: nrastogi@prl.res.in.

ORCID

Neeraj Rastogi: 0000-0003-4532-7827

Notes

The authors declare no competing financial interest.

■ ACKNOWLEDGMENTS

We thank Mr. Anil Mandaria and Mr. Abhishek Chakraborty for their help in sampling and analysis. S.T. acknowledges partial support from Department of Science and Technology, Govt. of India under the DST-UKEIRI project (reference no.: DST/INT/UK/P-144/2016).

■ REFERENCES

(1) Jacobson, M. C.; Hansson, H. Organic atmospheric aerosols: Review and state of the science. *Rev. Geophys.* **2000**, *38*, 267−294.

(2) Jimenez, J. L.; Canagaratna, M. R.; Donahue, N. M.; Prevot, a. S. H.; Zhang, Q.; Kroll, J. H.; DeCarlo, P. F.; Allan, J. D.; Coe, H.; Ng, N. L.; et al. Evolution of organic aerosols in the atmosphere. *Science* **2009**, *326* (5959), 1525−1529.

(3) Yang, M.; Howell, S. G.; Zhuang, J.; Huebert, B. J. Attribution of aerosol light absorption to black carbon, brown carbon, and dust in China-interpretations of atmospheric measurements during EAST-AIRE. *Atmos. Chem. Phys. Discuss.* **2008**, *8* (2), 10913−10954.

(4) Hecobian, A.; Zhang, X.; Zheng, M.; Frank, N.; Edgerton, E. S.; Weber, R. J. Water-soluble organic aerosol material and the light-absorption characteristics of aqueous extracts measured over the southeastern United States. *Atmos. Chem. Phys.* **2010**, *10* (13), 5965−5977.

(5) Kirchstetter, T. W.; Thatcher, T. L. Contribution of organic carbon to wood smoke particulate matter absorption of solar radiation. *Atmos. Chem. Phys.* **2012**, *12* (14), 6067−6072.

(6) Budisulistiorini, S. H.; Riva, M.; Williams, M.; Chen, J.; Itoh, M.; Surratt, J. D.; Kuwata, M. Light-Absorbing Brown Carbon Aerosol Constituents from Combustion of Indonesian Peat and Biomass. *Environ. Sci. Technol.* **2017**, *51*, 4415−4423.

(7) Laskin, A.; Laskin, J.; Nizkorodov, S. A. chemistry of atmospheric brown carbon. *Chem. Rev.* **2015**, *115* (10), 4335−4382.

(8) Feng, Y.; Ramanathan, V.; Kotamarthi, V. R. Brown Carbon: A Significant atmospheric absorber of solar radiation. *Atmos. Chem. Phys.* **2013**, *13* (17), 8607−8621.

DOI: 10.1021/acs.est.7b00734
Environ. Sci. Technol. 2017, 51, 6765−6772

(9) Arola, A.; Schuster, G. L.; Pitkänen, M. R. A.; Dubovik, O.; Kokkola, H.; Lindfors, A. V.; Mielonen, T.; Raatikainen, T.; Romakkaniemi, S.; Tripathi, S. N.; Lihavainen, H. Direct radiative effect by brown carbon over the Indo-Gangetic Plain. *Atmos. Chem. Phys.* **2015**, *15* (22), 12731−12740.
(10) Lin, G.; Penner, J. E.; Flanner, M. G.; Sillman, S.; Xu, L.; Zhou, C. Radiative forcing of organic aerosol in the atmosphere and on snow: Effects of SOA and brown carbon. *J. Geophys. Res. Atmos.* **2014**, *119* (12), 7453−7476.
(11) Graber, E. R.; Rudich, Y. Atmospheric HULIS: how humic-like are they? A comprehensive and critical review. *Atmos. Chem. Phys. Discuss.* **2005**, *5* (5), 9801−9860.
(12) Ervens, B.; Turpin, B. J.; Weber, R. J. Secondary organic aerosol formation in cloud droplets and aqueous particles (aqSOA): A review of laboratory, field and model studies. *Atmos. Chem. Phys.* **2011**, *11* (21), 11069−11102.
(13) Lin, P.; Laskin, J.; Nizkorodov, S. A.; Laskin, A. Revealing brown carbon chromophores produced in reactions of methylglyoxal with ammonium sulfate. *Environ. Sci. Technol.* **2015**, *49* (24), 14257−14266.
(14) Moise, T.; Flores, J. M.; Rudich, Y. Optical Properties of Secondary Organic Aerosols and Their Changes by Chemical Processes. *Chem. Rev.* **2015**, *115* (10), 4400−4439.
(15) Zhao, R.; Lee, A. K. Y.; Huang, L.; Li, X.; Yang, F.; Abbatt, J. P. D. Photochemical processing of aqueous atmospheric brown carbon. *Atmos. Chem. Phys.* **2015**, *15*, 6087−6100.
(16) Aggarwal, P. K.; Joshi, P. K.; Ingram, J. S. I.; Gupta, R. K. Adapting food systems of the Indo-Gangetic Plains to global environmental change: Key information needs to improve policy formulation. *Environ. Sci. Policy* **2004**, *7* (6), 487−498.
(17) Rastogi, N.; Singh, A.; Singh, D.; Sarin, M. M. Chemical characteristics of PM2.5 at a source region of biomass burning emissions: Evidence for secondary aerosol formation. *Environ. Pollut.* **2014**, *184*, 563−569.
(18) Shamjad, P. M.; Tripathi, S. N.; Pathak, R.; Hallquist, M.; Arola, A.; Bergin, M. H. Contribution of brown carbon to direct radiative forcing over the Indo-Gangetic Plain. *Environ. Sci. Technol.* **2015**, *49* (17), 10474−10481.
(19) Singh, A.; Rastogi, N.; Patel, A.; Satish, R. V.; Singh, D. Size-Segregated Characteristics of carbonaceous aerosols over the north-western Indo-Gangetic Plain: Year Round Temporal Behavior. *Aerosol Air Qual. Res.* **2016**, *16* (7), 1615−1624.
(20) Ramachandran, S.; Rengarajan, R.; Sarin, M. M. Atmospheric carbonaceous aerosols: Issues, radiative forcing and climate impacts. *Curr. Sci.* **2009**, *97* (1), 18−20.
(21) Census of India 2011. Primary census abstract - Data Highlights. *Prim. Census Abstr.* **2011**, 1−27 10.1017/CBO9781107415324.004.
(22) United states environmental protection agency. National ambient air quality standards. 2012, *826* (August 2014), 1−18.
(23) Kaul, D. S.; Gupta, T.; Tripathi, S. N.; Tare, V.; Collett, J. L. Secondary organic aerosol: A comparison between foggy and non-foggy days. *Environ. Sci. Technol.* **2011**, *45* (17), 7307−7313.
(24) Rai, P.; Chakraborty, A.; Mandariya, A. K.; Gupta, T. Composition and source apportionment of PM1 at urban site Kanpur in India using PMF coupled with CBPF. *Atmos. Res.* **2016**, *178−179*, 506−520.
(25) Updyke, K. M.; Nguyen, T. B.; Nizkorodov, S. A. Formation of Brown Carbon via Reactions of Ammonia with Secondary Organic Aerosols from Biogenic and Anthropogenic Precursors. *Atmos. Environ.* **2012**, *63*, 22−31.
(26) Yan, C.; Zheng, M.; Sullivan, A. P.; Bosch, C.; Desyaterik, Y.; Andersson, A.; Li, X.; Guo, X.; Zhou, T.; Gustafsson, Ö; Collett, J. L., Jr Chemical characteristics and light-absorbing property of water-soluble organic carbon in Beijing: Biomass burning contributions. *Atmos. Environ.* **2015**, *121*, 4−12.
(27) Teich, M.; van Pinxteren, D.; Wang, M.; Kecorius, S.; Wang, Z.; Müller, T.; Mocnik, G.; Herrmann, H. Contributions of nitrated aromatic compounds to the light absorption of water-soluble and particulate brown carbon in different atmospheric environments in Germany and China. *Atmos. Chem. Phys.* **2017**, *17*, 1653−1672.
(28) Powelson, M. H.; Espelien, B. M.; Hawkins, L. N.; Galloway, M. M.; De Haan, D. O. Brown carbon formation by aqueous-phase carbonyl compound reactions with amines and ammonium sulfate. *Environ. Sci. Technol.* **2014**, *48* (2), 985−993.
(29) Rastogi, N.; Patel, A.; Singh, A.; Singh, D. Diurnal variability in secondary organic aerosol formation over the Indo-Gangetic Plain during winter using online measurement of water-soluble organic carbon. *Aerosol Air Qual. Res.* **2015**, *15* (6), 2225−2231.
(30) Lukács, H.; Gelencser, A.; Hammer, S.; Puxbaum, H.; Pio, C. A.; Legrand, M.; Kasper-Giebl, A.; Handler, M.; Limbeck, A.; Simpson, D.; Preunkert, S. Seasonal trends and possible sources of brown carbon based on 2-year aerosol measurements at six sites in Europe. *J. Geophys. Res.* **2007**, *112* (23), 1−9.
(31) Aiken, A. C.; DeCarlo, P. F.; Jimenez, J. L. Elemental analysis of organic species with electron ionization high-resolution mass spectrometry. *Anal. Chem.* **2007**, *79* (21), 8350−8358.
(32) Li, Y. J.; Lee, B. Y. L.; Yu, J. Z.; Ng, N. L.; Chan, C. K. Evaluating the degree of oxygenation of organic aerosol during foggy and hazy days in Hong Kong using high-resolution time-of-flight aerosol mass spectrometry (HR-ToF-AMS). *Atmos. Chem. Phys.* **2013**, *13* (17), 8739−8753.
(33) Chakraborty, A.; Gupta, T.; Tripathi, S. N. Combined effects of organic aerosol loading and fog processing on organic aerosols oxidation, composition, and evolution. *Sci. Total Environ.* **2016**, *573*, 690−698.
(34) Rajput, P.; Gupta, T.; Kumar, A. Diurnal variability of sulfate and nitrate aerosols during wintertime in the Indo-Gangetic Plain: Implications to heterogeneous phase chemistry. *RSC Adv.* **2016**, *6*, 89879−89887.
(35) Zhang, X.; Lin, Y. H.; Surratt, J. D.; Weber, R. J. Sources, composition and absorption angström exponents exponent of light-absorbing organic components in aerosol extracts from the los angeles basin. *Environ. Sci. Technol.* **2013**, *47* (8), 3685−3693.
(36) Srinivas, B.; Rastogi, N.; Sarin, M. M.; Singh, A.; Singh, D. Mass absorption efficiency of light absorbing organic aerosols from source region of paddy-residue burning emissions in the Indo-Gangetic Plain. *Atmos. Environ.* **2016**, *125*, 360−370.
(37) Kirillova, E. N.; Andersson, A.; Han, J.; Lee, M.; Gustafsson, Ö. Sources and light absorption of water-soluble organic carbon aerosols in the outflow from northern China. *Atmos. Chem. Phys.* **2014**, *14* (3), 1413−1422.
(38) Cheng, Y.; He, K. B.; Zheng, M.; Duan, F. K.; Du, Z. Y.; Ma, Y. L.; Tan, J. H.; Yang, F. M.; Liu, J. M.; Zhang, X. L.; et al. Mass absorption efficiency of elemental carbon and water-soluble organic carbon in Beijing, China. *Atmos. Chem. Phys.* **2011**, *11* (22), 11497−11510.
(39) Zhong, M.; Jang, M. Dynamic light absorption of biomass-burning organic carbon photochemically aged under natural sunlight. *Atmos. Chem. Phys.* **2014**, *14* (3), 1517−1525.
(40) Liu, J.; Scheuer, E.; Dibb, J.; Diskin, G. S.; Ziemba, L. D.; Thornhill, K. L.; Anderson, B. E.; Wisthaler, A.; Mikoviny, T.; Devi, J. J.; et al. Brown carbon aerosol in the north American continental troposphere: Sources, abundance, and radiative forcing. *Atmos. Chem. Phys.* **2015**, *15* (14), 7841−7858.
(41) Kirchstetter, T. W.; Novakov, T.; Hobbs, P. V. Evidence that the spectral dependence of light absorption by aerosols is affected by organic carbon. *J. Geophys. Res. D Atmos.* **2004**, *109* (21), 1−12.
(42) Desyaterik, Y.; Sun, Y.; Shen, X.; Lee, T.; Wang, X.; Wang, T.; Collett, J. L. Speciation of "brown" carbon in cloud water impacted by agricultural biomass burning in eastern China. *J. Geophys. Res. Atmos.* **2013**, *118* (13), 7389−7399.
(43) Lin, P.; Liu, J.; Shilling, J. E.; Kathmann, S. M.; Laskin, J.; Laskin, A. Molecular characterization of brown carbon (BrC) chromophores in secondary organic aerosol generated from photo-oxidation of toluene. *Phys. Chem. Chem. Phys.* **2015**, *17* (36), 23312−23325.
(44) Wang, X.; Heald, C. L.; Ridley, D. A.; Schwarz, J. P.; Spackman, J. R.; Perring, A. E.; Coe, H.; Liu, D.; Clarke, A. D. Exploiting simultaneous observational constraints on mass and absorption to

DOI: 10.1021/acs.est.7b00734
Environ. Sci. Technol. 2017, 51, 6765−6772

estimate the global direct radiative forcing of black carbon and brown carbon. *Atmos. Chem. Phys.* **2014**, *14* (20), 10989−11010.
(45) Di Lorenzo, R. A.; Washenfelder, R. A.; Attwood, A. R.; Guo, H.; Xu, L.; Ng, N. L.; Weber, R. J.; Baumann, K.; Edgerton, E.; Young, C. J. Molecular-Size-Separated Brown Carbon Absorption for Biomass-Burning Aerosol at Multiple Field Sites. *Environ. Sci. Technol.* **2017**, *51*, 3128.

DOI: 10.1021/acs.est.7b00734
Environ. Sci. Technol. 2017, 51, 6765−6772